DESIGN AND INITIAL TEST OF ONR SUPERCAVITATING HYDROFOIL BOAT XCH-6

Glen J. Wennagel
Dynamic Developments, Inc.
Babylon, New York

INTRODUCTION

The Grumman Aircraft Engineering Corp. and its affiliate, Dynamic Developments, Inc., are engaged in research and development programs directed toward practical, high-speed hydrofoil systems. Emphasis is placed on application to vehicles with water speeds between 50 and 100 knots. Three of the test programs which assist in this effort are considered to be of special interest to the Third Symposium on Naval Hydrodynamics. The first of these programs utilizes a whirling tank facility which enables hydrodynamic and hydroelastic tests on waterborne or underwater devices up to speeds of 100 knots. The second program utilizes a pendulum facility wherein hydrodynamic models swing through a water tank of variable water temperature and, consequently, variable vapor pressure.

The third test program utilizes a research and test craft with supercavitating surface-piercing hydrofoils, a supercavitating propeller and a gas turbine power plant. This vehicle has been chosen as the subject for discussion herein. Construction and initial tests have been performed under Contract Nonr 2695(00) with the Office Of Naval Research. The purpose of this test program is to determine the hydrodynamic efficiencies of the propeller and hydrofoil system over a speed range between 0 and 60 knots, and to investigate corrosion preventive measures for gas turbine engines operating in a marine environment.

GENERAL CHARACTERISTICS

General characteristics of the craft are shown in Figs. 1, 2a, 2b, and 2c. Overall length, with foils extended, is 23.3 feet. Clearance between the keel and the 60.0-knot water line is 2.08 feet. Takeoff gross weight, with one pilot, is 2550 pounds. Table 1 gives a complete weight statement.

HULL

The hull has been constructed from an aluminum sport boat manufactured by Grumman Boats, Inc. Three primary modifications have been made to the basic hull. The first is the addition of Lockfoam covered with three layers of fiberglass cloth to the forebody bottom. The new forebody lines were established through the addition of ribs installed external to

646551 O—62——15

Fig. 1. The ONR supercavitating hydrofoil boat

the original hull. This addition increases forebody deadrise, so as to minimize wave impact loads on the hull, and forms a step on the hull bottom. Vertical tubes are installed within the boat and through the hull bottom aft of the step, to facilitate step ventilation. A second modification is an aluminum box aft of the transom of the basic boat which gives the craft a desired overall length and provides support for the tail hydrofoil and strut assembly. The third modification is an opening for the engine exhaust in the starboard side-skin near the aft end of the basic hull. Stainless steel sheet is used as a doubler around this cutout to provide strength over a region affected by the high temperatures of the exhaust.

The basic hull skin is fabricated by stretch-forming two pieces of sheet which are joined together at the keel. Riveted construction is employed to attach hull and box extension skins to ribs and longitudinal stiffeners. All the aluminum is 61S-T6 alloy.

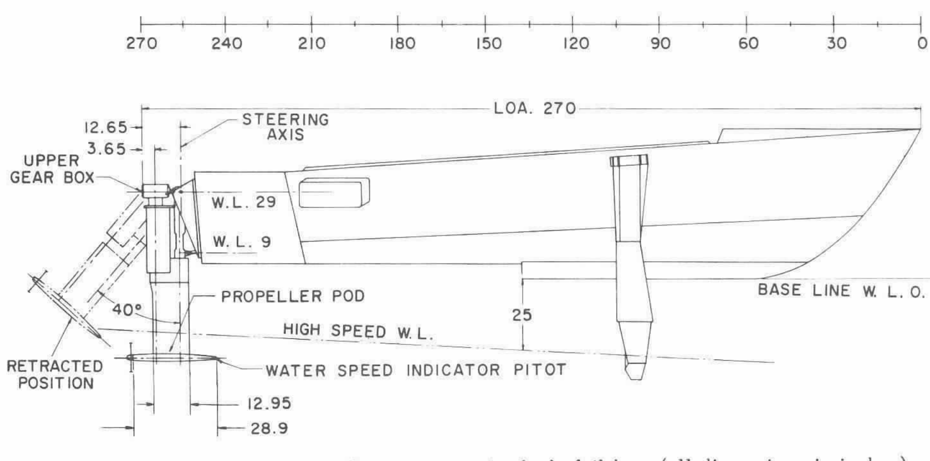

Fig. 2a. Side view of the ONR supercavitating hydrofoil boat (all dimensions in inches)

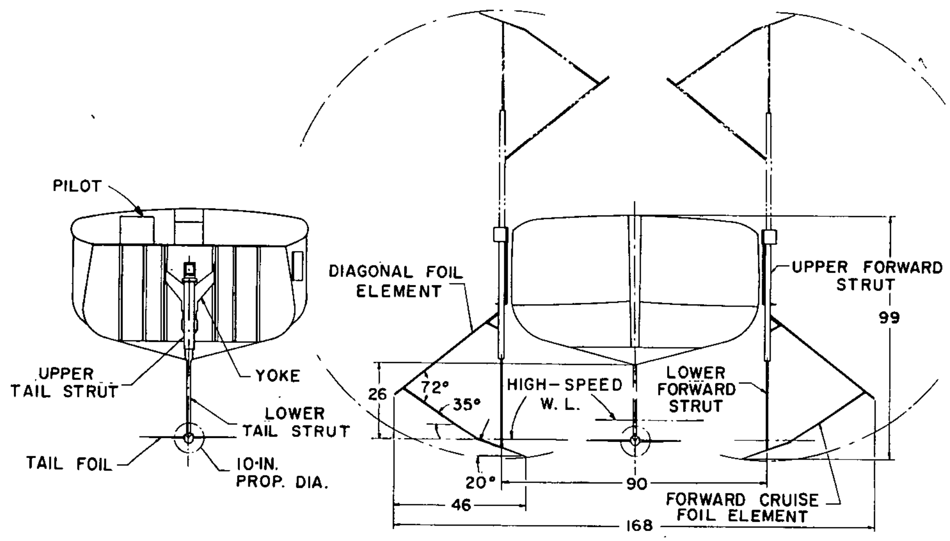

Fig. 2b. Front and rear views of the ONR supercavitating hydrofoil boat

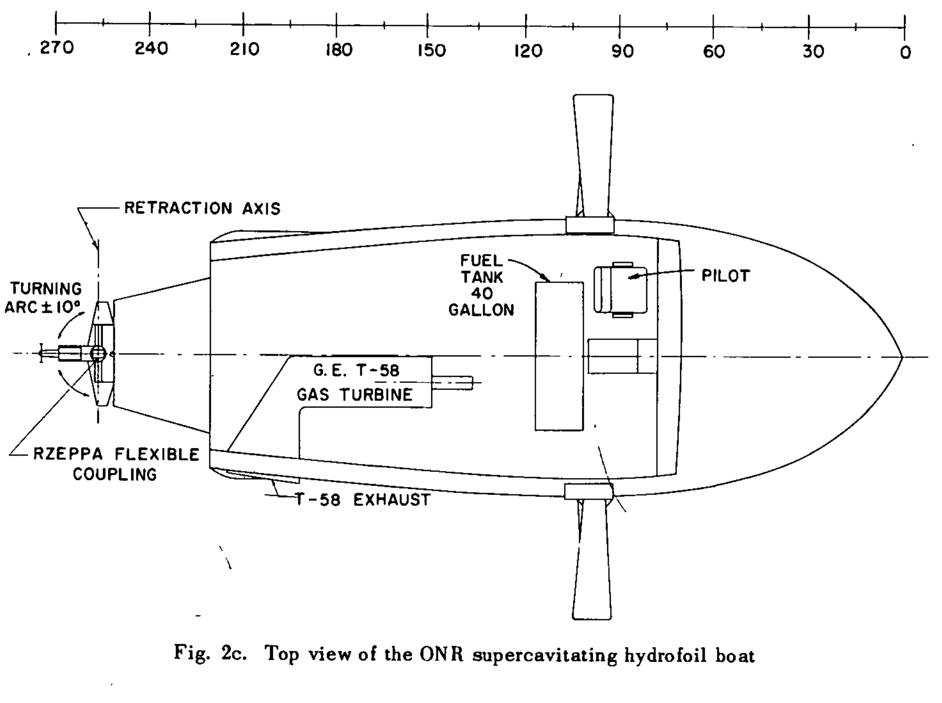

Fig. 2c. Top view of the ONR supercavitating hydrofoil boat

Table 1
Weight Statement

Item	Weight (lb)	
Hull:		709
Basic Boat	425	
Forebody Bottom Addition	130	
Aft Box Extension	105	
Step Vent Tubes	14	
Pilot Seat and Supports	35	
Forward Foil Assemblies and Supports:		392
Support Fittings and Structure	80	
Upper Struts	94	
Lower Struts	64	
Diagonal Foils	84	
Cruise Foils	70	
Tail Foil Assembly:		155
Tail Strut	43	
Yoke	32	
Strut and Yoke Support Fittings	37	
Propeller Pod	25	
Upper Gear Box	12	
Tail Foil	6	
Transmission (All Gears, Shafting, Bearings, Seals, Couplings):		117
Powerplant:		598
General Electric T-58 and Reduction Box	375	
Engine Mounts	78	
Exhaust Duct and Hull Supports	60	
Bellmouth and Screen	10	
Cowl and Supports	15	
Throttle Control and Supports	15	
Tachometers and Throttle Slave	10	
Engine Instruments and Panel	35	
Lubrication and Fuel System:		211
Pumps	19	
Fuel and Oil	92	
Fuel Tank and Supports	10	
Oil Tanks (2) and Supports	41	
Fuel and Oil Lines	34	
Fuel (1) and Oil (2) Filters	15	
Steering System		42
Lear Actuator (For Tail Strut Incidence Adjustment)		13
Pilot and Equipment		210
Torquemeter		15
Air Bleed System		15
Battery		53
Propeller		10
Miscellaneous		10
Total		2550

HYDROFOIL SYSTEM

Two surface-piercing hydrofoils (one on each side of the boat) are located forward of the vehicle center of gravity and one fully submerged foil is located aft of the transom. Approximately 77.0 percent of the vehicle weight is supported on the forward hydrofoils.

As seen in Fig. 3, each of the forward hydrofoil assemblies incorporates a vertical strut supported to the hull in its upper region. A cruise foil element is attached to the lower end of each strut. A portion of this element is cantilevered so as to extend inboard of the strut bottom. In addition, it extends outboard and up from the lower end of the strut with positive dihedral. The upper end of each cruise foil is joined to the upper region of the strut by a diagonal foil element with negative dihedral.

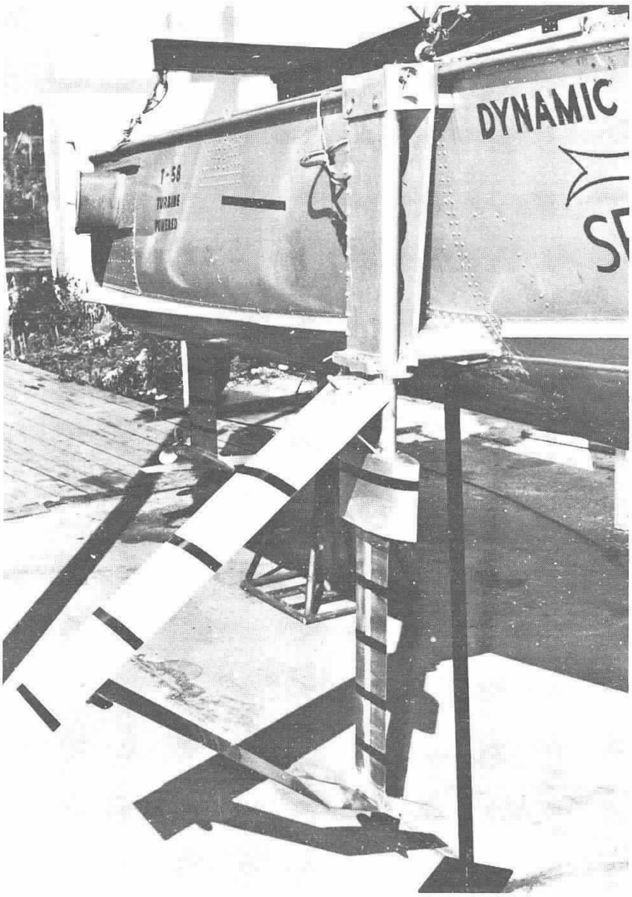

Fig. 3. A forward hydrofoil assembly

Cross sections of the foil and strut elements of the forward foil assembly are shown in Fig. 4. The cruise foil elements embody a basic supercavitating section which has a circular-arc bottom shape, a flat upper contour, a sharp leading edge, and a blunt trailing

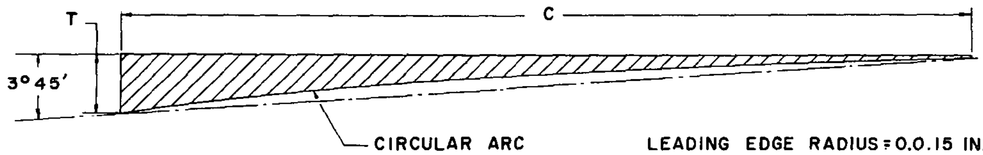

FORWARD CRUISE FOIL SECTION
R=RADIUS OF UPPER SURFACE CONTOUR

LOCATION	C IN.	T IN.	R IN.
OUTBOARD END	11.940	0.811	177.733
DIHEDRAL BREAK	8.394	0.578	124.688

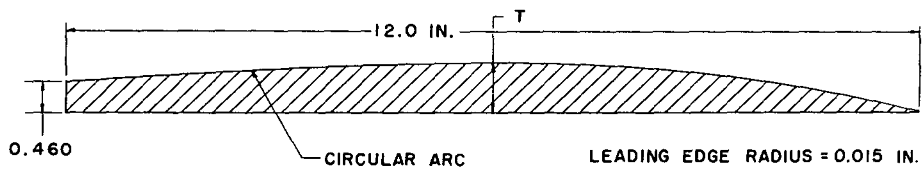

FORWARD DIAGONAL FOIL SECTION
R = RADIUS OF UPPER SURFACE CONTOUR

LOCATION	T IN.
OUTBOARD TIP	0.72
INBOARD END	1.20

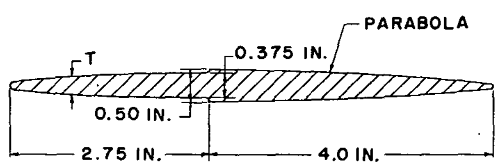

TRAILING EDGE RADIUS = 0.062 IN.

LOWER FORWARD STRUT SECTION

PERCENT CHORD	T IN.
60.1	0.375
81.5	0.375
92.7	0.260

Fig. 4. Cross sections of the elements of a forward hydrofoil assembly

edge. Over the lower regions of this element, a tapered afterbody is added to the basic section. At low speeds, prior to cavity formation, this afterbody reduces the drag which would exist for the basic section. At higher speeds, after cavity formation, the afterbody is essentially unwetted but still contributes to section strength and stiffness. The diagonal foil elements, which are wetted only during low-speed operation, employ a subcavitating cross section with a vented base. This section employs a flat bottom, a circular-arc upper contour, a sharp leading edge, and a blunt trailing edge. The strut cross section employs a parabolic forebody and a tapered afterbody; the two regions of this section are separated by a step.

The tail hydrofoil (Fig. 5) employs zero dihedral and is supported on the forward half of the propeller pod; the pod is supported by a single strut. Figure 6 illustrates the strut and foil cross sections. The tail hydrofoil section is of symmetrical, subcavitating design and incorporates a low thickness ratio. A parabolic cross section with a blunt base is used on the tail strut. Propeller pod fineness ratio is approximately 8.5.

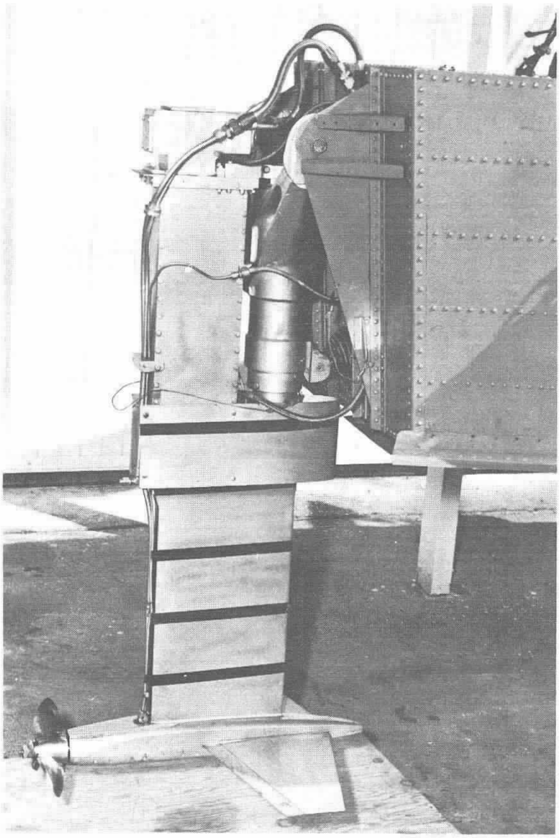

Fig. 5. The tail strut, propeller, and hydrofoil

The forward, cruise foil elements and lower struts are fabricated from solid stainless steel. Upper regions of the forward and tail struts are fabricated from heavy-gage aluminum plate. Diagonal foils, tail foil, lower tail strut, and propeller pod are machined from solid aluminum.

Each forward, cruise foil element is attached to its supporting strut by flush-head bolts which are inserted from the bottom side of each foil element and which extend into tapped holes of the struts. Diagonal to cruise element attachment is similar, with bolt

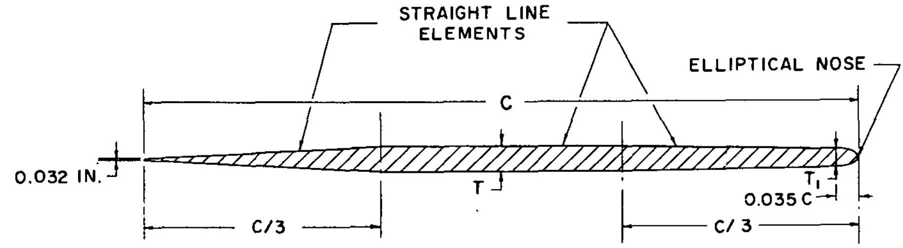

TAIL FOIL SECTION
ALL INTERSECTIONS OF STRAIGHT LINE ELEMENTS ARE ROUNDED

LOCATION	C IN.	
ROOT	13.00	T = 0.0375 C
OUTBOARD TIP	3.66	T_1 = 0.0254 C

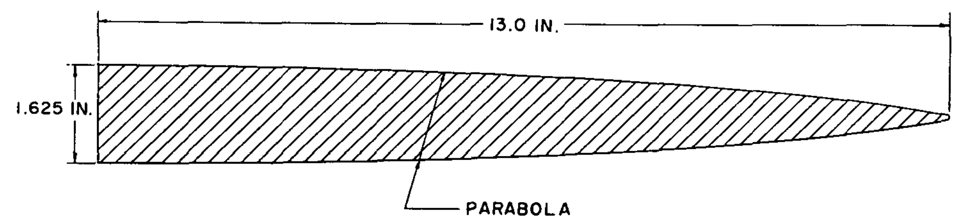

TAIL STRUT SECTION

Fig. 6. Cross sections of the tail strut and hydrofoil

insertion from the upper side of each diagonal and with tapped holes in each cruise foil element. These intersections are thus maintained hydrodynamically clean without resort to bodies of revolution. Diagonal to upper strut connection on each forward foil assembly involves one fitting and connecting bolts. Each of the two lower struts extends up into an adjoining, hollow, upper strut; attaching bolts connect the mating segments. This design enables easy replacement or modification of any of the four, separate components which make up each forward hydrofoil assembly.

The propeller pod is split along a horizontal plane so as to form an upper half and a lower half. Suitable machining allows for the insertion of a one-piece tail foil between the upper and lower halves of the pod. Attaching bolts, which are externally flush, connect these three structural elements. Thus, emphasis has been placed on obtaining a design which allows easy replacement or modification of the tail hydrofoil.

A welded connection is employed between the upper half of the pod and the tail strut. This welding extends around the entire perimeter of the strut cross section and has been hand polished to obtain a smooth finish. Rigid and fixed connection between these two elements was a design requirement so as to allow subsequent, internal machining of both strut and pod in a manner that could guarantee proper alignment of transmission components.

An upper tail strut, of hollow construction, attaches to the top of the lower strut, and provides support at its upper end for a right-angle gear box. Gear box and lower strut attachment is by bolts to allow easy disassembly and inspection of internal transmission components.

All aluminum components are 61S-T6 alloy; all steel elements are 416 stainless alloy with an ultimate tensile strength of 150,000 psi. The struts, which employ constant cross section, were externally contoured by a single pass through a Whaley Machine of 14-inch diameter. A Keller BL Model C Machine was used for obtaining the more complicated external contours of the forward cruise hydrofoils.

CONTROLS AND RETRACTION

The boat is steered by rotation in yaw of the entire tail strut-pod-foil assembly. Tail foil incidence with respect to the keel is adjustable while foilborne, and a trailing edge trim tab is provided on the cruise foil element of one forward hydrofoil assembly. Each of the three hydrofoil assemblies is separately retractable.

Tail assembly retraction, steering, and incidence adjustment in pitch are accomplished by means of a unique, structural yoke. The yoke is an aluminum casting with machined surfaces. As shown in Fig. 2a, the yoke provides support to the tail strut at two, vertically separated locations. Both of these supports are through sleeve bearings on cylindrical portions of the yoke structure. The bearings, in turn, support an aluminum tube which is rigidly bolted to the strut assembly at both support points. The sleeve bearings allow rotation of the tail assembly in yaw, about the tube and steering axis. This axis, extended, coincides with the 20.0-percent chord line of the lower strut. Each of the bearings can transmit loads in a horizontal plane. Up and down loads are transferred from the tube to the yoke at the lower and upper bearing supports, respectively. The upper end of the tube and the top of the strut are joined by a fitting. This fitting supports the upper gear box and has an arm extending out on its port side. Connected to the arm is a fore and aft push-pull rod of the steering system. Rod loads establish equilibrium of the tail assembly in regard to moments applied about the steering axis and motion of the rod provides steering action. Strut displacement in yaw is limited by stops to plus or minus 6.0 degrees. The remainder of the steering system provides for mechanical, irreversible control from the pilot's wheel. At high speed, only small strut rotations are required; a wheel-to-strut rotation ratio of 54.5 to 1.0 is employed.

Yoke support to the hull is provided at three pickup points. Two points at the upper end of the yoke, separated athwartship, are hinged on a lateral axis. Rotation about this axis allows for both retraction and for tail foil incidence adjustment. Each of the two upper support points can transmit loads in all directions. The third support point is at the bottom of the yoke and is attached to the hull through an electrically operated, linear actuator manufactured by Lear, Inc., Instrument Division, Stamford, Connecticut (Model No. 434-AJ). Variable length of this support, in the fore and aft direction, allows incidence change in pitch while foilborne. This attachment is designed to take only axial (fore and aft) loads.

The vertical steering axis and the lateral retraction axis intersect at a point on the vehicle vertical plane of symmetry. Also passing through this point is the centerline of longitudinal, transmission shafting. A Rzeppa coupling in the transmission, at this three-axis intersection, allows for simultaneous transmission of power, tail assembly incidence change in pitch, and tail assembly steering. Manufacture of the flexible coupling is by Dana Corp., Con-Vel Division, Detroit, Michigan (Model No. OR).

Three pickup points on the hull support each upper strut of the forward foil assemblies. Two points on top of each strut, separated in the fore and aft direction, are hinged on a longitudinal axis. Each of these supports can take loads in all directions. A third support on each strut is located at the chine. It consists of a manually operated, locking handle which can take loads in the lateral direction only. When this latter support is unlocked, each forward foil assembly can be retracted by rotation outboard and up.

Provision has been made to avoid damage to the primary hull structure in case the hydrofoils strike a solid object. On the forward foil assemblies, shear pins which attach the support fittings, on top of the upper struts, to the upper struts are designed to fail under specific loads. In the event of a failure, the affected forward assembly can leave the vehicle in the aft direction; the support at the locking handle, near the chine, allows this motion without restraint. On the tail assembly, retraction can occur, under a crash condition, by means of a shear pin incorporated in the lower yoke support and designed to fail under a specified load. In the event of such failure, damage would be localized to the Rzeppa coupling in the longitudinal transmission shafting.

A manually operated, trailing edge trim tab is installed on the cruise foil element of the starboard forward foil assembly. It allows trim of the vehicle in roll.

TRANSMISSION

Line shafting runs aft from the engine to the upper gear box, down through the tail strut to the propeller pod and then aft to the propeller. The transmission arrangement is shown in Fig. 7. Precise design and manufacture has achieved a rigid design criteria of minimum frontal area on the strut and pod. At 200 hp and at the maximum output speed of the engine reduction box, 6000 rpm, gears and bearings are designed for a 50-hour life. Design and manufacture was by the Medium Steam Turbine and Gear Division, General Electric Company, Lynn, Massachusetts.

Shafting between the engine and upper gear box incorporates a torque sensor, a torque limiting shear pin and couplings with bearing supports. At the intersection of the transmission, retraction, and steering axes, a Rzeppa coupling allows both angular misalignment and parallel offset of shaft centerlines.

Upper gear box and pod each contain a right-angle, spiral bevel gear set of 1.0 to 1.0 ratio wherein each gear incorporates a 35-degree spiral angle and a 20-degree pressure angle. They are of 3.0-inch pitch diameter and 7.0 diametral pitch. All gears are keyed to their respective shafts except for the pod pinion which has a major diameter fit fixed spline and a rear face which shoulders against its drive shaft. Material is AISI-9310 aircraft quality stock. Teeth were case-carburized to 60-63 RC after generating and then finish ground. The gears were developed with proper contact patterns on both sides of the teeth so that a single grinder set up could produce the gearing for both the upper and pod bevel sets.

Connection between the upper gear box and the pod pinion drive shaft is made by a free-floating, internally splined quill shaft in the upper strut. A ball bearing carries the thrust reaction of the pod pinion, and this bearing has been located in an area well above the high-speed water line where sufficient housing volume is available without detrimental effect on drag. The length of the drive shaft between the thrust bearing and the pod pinion is approximately 26.0 inches. Pod pinion radial reactions are carried by precision needle bearings. The pinion drive shaft is induction-hardened and ground in the locale of these needle bearings to serve as integral bearing races; this feature acts to further reduce frontal area. The pod pinion's axial load component was selected to be of minimum value

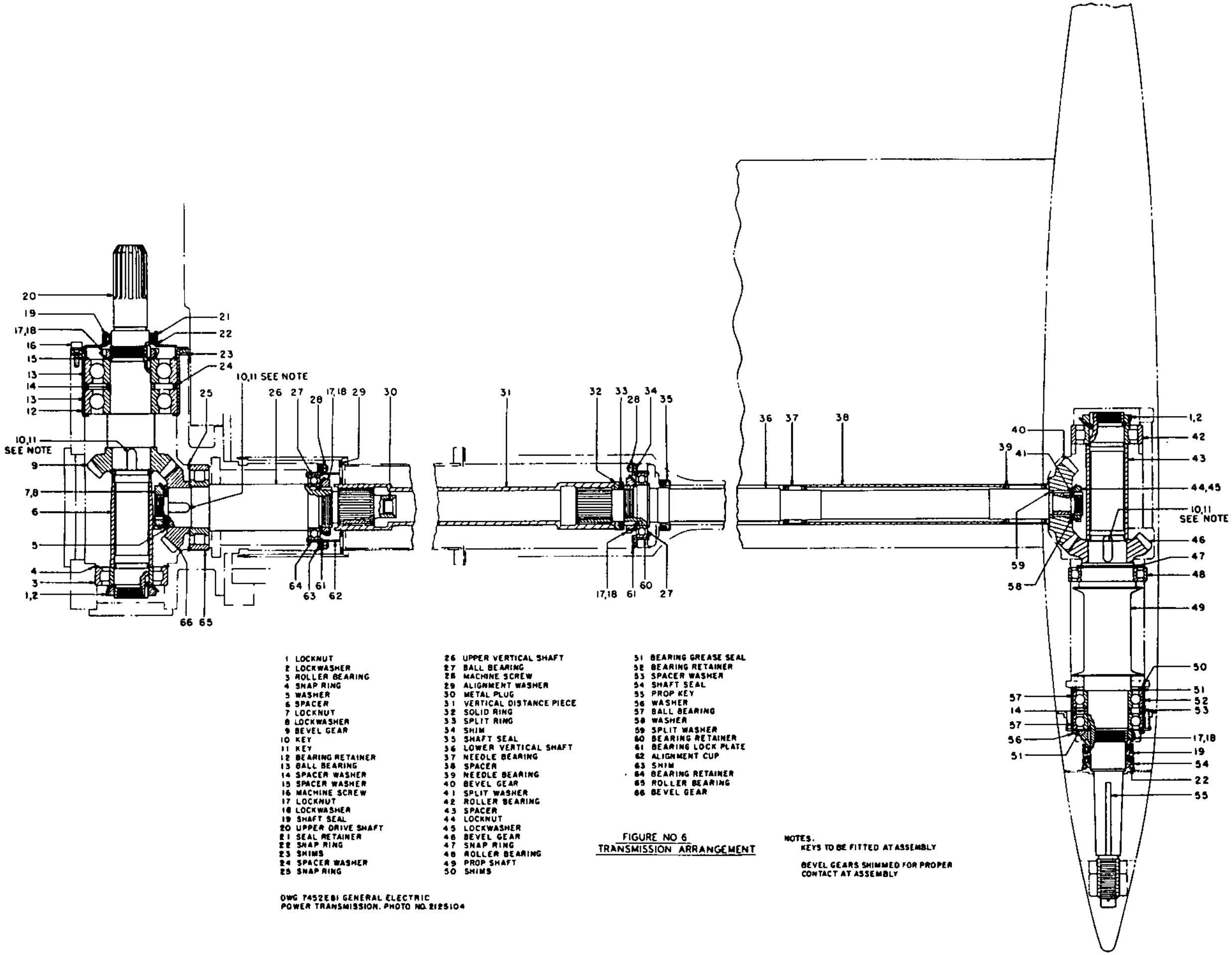

Fig. 7. The transmission arrangement

while the gear's axial component is of maximum value. The hand of the spiral angle is such that the gear's axial reaction is out of mesh, or to the rear, in direct opposition to the propeller thrust. This allowed for the use of relatively small propeller shaft thrust bearings, since the net bearing thrust load is the difference of these forces. Two thrust bearings are employed just forward of the propeller shaft seals. Two roller bearings straddle-mount the gear to provide radial reactions.

Shafting in the upper gear box and the quill shaft are of 4340 stock with induction-hardened splines. The pod pinion drive shaft is of 4350 stock while the propeller shaft is of forged and age-hardened K-monel. The areas of seal contact on the transmission input shaft and propeller shaft are built up with a copper flash followed by a nickel flash and a hard chrome plate.

Seals are of the double lip type and made of Sirvene 7080, a material chosen for its sea-water resistance. A single seal is used at the drive input with system lube oil depended upon for lubrication. Tandem seals packed with a sea-water-resistant grease are used on the propeller shaft. An interesting feature is that the pod structure is split horizontally along its longitudinal axis and bolted together on assembly. The pod machinery area is sealed by filling a machined groove, which runs along the periphery of each half, with a room-temperature self-curing, silicone rubber compound.

Damage due to galvanic action has been controlled by careful selection of materials exposed to sea water. Like the propeller shaft, the pod seal carrier is of K-monel. A locking ring, used to retain the seals, is cadmium plated. All lube and scavenge fittings and lube oil supply lines and grease fittings are of aluminum. To date, there is no evidence of erosion due to galvanic action.

The lubricant used conforms to specification MIL-0-6086 (light). This is a petroleum-base aircraft gear oil containing extreme pressure additives. An electric pump in the lube supply system delivers two quarts of oil per minute at 20 psig. A pressure sensing switch has been incorporated in the supply line. If the pressure falls below 15 psig, this switch opens a return line from the engine fuel control to the fuel tank and engine shutdown is thereby automatic. A panel light then goes on to inform the pilot of the reason for engine shutdown. Total oil flow is divided by a tee located at the boat transom so that one quart per minute is supplied both to the upper gear set and to the pod gearset. Gear mesh and input shaft thrust bearings are pressure-lubricated in the upper gear box. Oil mist and oil flow by gravity lubricate the remaining gear box bearings, the spline couplings of the quill shaft, and the thrust bearing of the pod pinion drive shaft. A single lip seal directly beneath the pod pinion thrust bearing prevents leakage of oil to the pod. An oil scavenge port is located at the level of this seal to allow the return of the lubricant to the lube system. Needle bearings for radial load reaction on the pod pinion drive shaft are grease packed on assembly, and a grease fitting is provided to the uppermost of these bearings. A spray nozzle, to pressure lubricate the pod gearset, is located at the aft end of the pod-strut juncture. Oil mist is depended upon to lubricate the propeller shaft roller bearings. The pod is bored to give the effect of a shroud about the driven bevel gear. Dual channels run axially from below the gear to a sump just forward of the foremost roller bearing. This sump is shrouded to break up windage effects from a roller bearing locknut. The lubricant is then scavenged through drilled passageways up through the strut where connection to the lube scavenge system is made. Propeller shaft thrust bearings are grease packed and are provided with ring seals. Wash out of the grease packing by lube oil is prevented by slinger rings on the propeller shaft. Scavenge lines are joined at the transom into one line which continues forward. An electric scavenge pump returns the lubricant to a reservoir. An oil cooler has been found unnecessary and is not used.

Magnetic drain plugs are employed in the strut and in the pod to provide indication of gear or bearing wear.

ENGINE

Power is supplied by a General Electric YT-58-2 free turbine engine. Maximum turbine output speed is 19,500 rpm. An engine gear box with a 3.25-to-1.0 ratio reduces the output shaft speed to a maximum of 6000 rpm. At this speed, the engine has a guaranteed normal continuous rating of 900 hp on a 59°F day and 765 hp at 80°. Although available power is greatly in excess of vehicle requirements, its light weight and desirable output speed make the T-58 particularly well suited for this application. Engine fuel and lubrication systems are in accord with normal practice for this engine, with 5-micron and 25-micron filters installed in the engine fuel and gear box oil supply lines, respectively.

A goal of this program has been to determine the location and degree of corrosion effects on engine components and to test thereafter various coatings and changes in material so as to systematically accomplish a final marinization of the YT-58-2 engine. Accordingly, initial installation utilized a standard engine, No. SN-200-103, without any special component protection, external cowling, or maintenance procedure.

External corrosion was first observed on small, unpainted areas of the engine's magnesium front frame and of the magnesium reduction gear box. Further corrosion was then prevented in these locations by a grease coating. Thereafter, stiffness became apparent in the linkage motion of the variable stator system. This stiffness was then corrected by periodic application of oil. Subsequent corrosion occurred on other exterior components. Again, after observation for a suitable period of time, further corrosion was halted in each locale by regular application of grease or oil.

Engine operation was continued, with inlet exposure to direct salt-water spray, until the turbine inlet temperature reading at idle had increased to approximately 100° C higher than normal. Removal of the compressor casing revealed a significant amount of corrosion throughout the entire compressor, with the effects of corrosion increasing toward the later stages. Although the aerodynamic configuration of the higher stage blading had been materially affected, engine starting difficulty had not been encountered. The compressor rotor was cleaned by hand using large, gun barrel brushes; blades were removed and cleaned with an aluminum oxide blast. The engine was reassembled and a cowling was installed to protect the inlet from direct salt-water spray. In addition, engine washdowns were begun whereby 2.5 gallons of fresh water were sprayed into the inlet just prior to engine shutdown after each test period. A second period of operation, equivalent to the first, was completed and internal engine components were again inspected. It was found that the simple procedures then adapted had essentially halted the spread of further corrosion. Engine temperatures and operation remained normal over the observation period.

A second engine, No. SN-200-102, has recently been installed and is currently being used during test operations. It is a modified engine intended to test the effectiveness of certain coatings in preventing corrosion of engine components. Table 2 gives a list of these components and their coatings. Prior to installation, test-stand operation was completed by the General Electric Company to determine the effects of these modifications on aerodynamic characteristics. They have been found small, and guaranteed performance ratings remain unchanged. Vehicle operation will continue to use engine washdowns, exterior oil application and inlet cowling. While no effects of corrosion have yet been observed with this engine, insufficient operating time has been accumulated to allow proper conclusions.

Table 2
Marinization Changes to the YT-58-2 Engine

Engine Dash No.*	Engine Item	Material and Specification No.	Coating or Treatment
102 and 101	Front Frame	Magnesium AMS 4434	Nubelon S
102 and 101	Compressor Casing	Steel, G. E. SAED B50T1131	Nickel Plate
102 and 101	Compressor Rear Frame	Steel, G. E. SAED B50T1131	Nickel Plate
102	Compressor Spool & Blade Assy	Steel AMS 6451	Nubelon S
102 and 101	Compressor Sta. Vanes & Rings	Steel AISI 405	....
	Stages 1 thru 7	....	Nubelon S
	Stages 8 and 9	....	Heresite
	Stage 10 and Exit Vanes	....	Silicone Alum.
102 and 101	Combustion Chamber Casing	Steel, G. E. SAED B50T1131	Nickel Plate
101	Variable Stator Actuating Rings	Steel AISI 410	Chrome Plate
101	Variable Stator Actuator Levers	Steel AMS 5120	Nickel Plate
101	Main Reduction Gear Case	Magnesium AMS 4434	Replace with Aluminum, Alodine
101	All Magnesium Engine Components	Magnesium AMS 4434	Replace with Aluminum, Alodine
101	Compressor Spool	Steel AM-355	Nubelon S

*This column identifies the changes as applying to the second engine, No. SN-200-102, or to the third engine, No. SN-200-101.

A third engine, No. SN-200-101, is being modified for later installation and test. It includes all of the coatings incorporated in the second engine, with additional changes as given in Table 2. It is hoped that this engine, after test-stand operation and waterborne service with suitable operating procedures, will represent a final marinization of the YT-58-2 engine.

PROPELLER

The propeller is located on the aft end of the propeller pod behind the tail foil and strut. It has been designed and manufactured by personnel of the David Taylor Model Basin for zero cavitation number and in accordance with the DTMB three-bladed, supercavitating propeller series. This series is fully described in Refs 1-3. Propeller diameter is 10.0 inches; pitch ratio at the 70.0 percent radius is 1.61; expanded area ratio is 0.457; blade thickness fraction is 0.024; rotation is clockwise looking forward. Propeller material is stainless steel with an ultimate tensile strength of 140,000 psi. A design feature is a nylon liner between the propeller hub and the propeller shaft. The shaft is tapered and propeller attachment is by means of a locknut and a brass key. Friction between the hub and shaft is reduced, by the nylon liner, to a very low value. This reduced friction, together with a torque limit on the locknut, has enabled specification of key size such that key failure in shear occurs at a predetermined value of propeller torque. Protection to transmission components is thereby provided for a condition wherein the propeller might strike floating debris or some solid object. Laboratory tests were undertaken to determine proper key size; failure of the key occurs at a torque of 2500 inch-pounds.

INSTRUMENTATION

Instrumentation has been incorporated to provide cockpit indication of water speed, propeller torque, propeller rotative speed, propeller thrust, keel trim in pitch, tail foil incidence in pitch with respect to the keel, tail strut position in yaw, transmission and engine oil temperatures and pressures, compressor and power turbine speeds and temperatures, and fuel pressure.

The propeller torque measuring device is installed in the horizontal transmission shaft aft of the engine gear box. It is a torque transducer, Model No. TG-5-3000A, manufactured by the Crescent Engineering and Research Company, El Monte, California. The core or sensor section of the transducer incorporates a solid shaft which acts as a torsional spring. It is splined at its ends to mating sections of the drive shaft, and is enclosed by a cylindrical, fixed pickup unit. Cylindrical crowns are attached to the shaft of the sensor section at two locations which are separated along its longitudinal axis. The crowns have intermeshing teeth which extend around the center region of the solid shaft. Torque causes a change in the size of air gaps which exist between the intermeshed teeth of the two crowns, and this change modifies the magnetic reluctance. The variation in reluctance effects proportional changes of impedance in two coils of the enclosing pickup unit. The coils perform as two legs of an ac bridge to reflect electrical unbalance which is proportional to torque. This unbalance is amplified, demodulated and applied to a microammeter which reads torque directly.

Propeller thrust is calculated by employing strain gages affixed to the linear actuator which attaches the lower yoke support point to the hull. Data is recorded on a portable oscillograph. Measured compression loads in the actuator enable the calculation of propeller thrust, as required for moment equilibrium about the retraction axis, based on estimated tail foil lift and tail assembly drag components, together with associated centers of pressure. The calculation of thrust is therefore approximate at the present time. It is planned to perform towing-tank tests of the tail assembly to accurately measure estimated quantities and to thereby provide more accurate calculation of propeller thrust.

FLOW CONDITIONS

Flow conditions involve cavities over the upper surface and behind the blunt base of each forward cruise foil, behind the blunt base of each forward diagonal foil, along the afterbody sides of the forward struts, and behind the blunt base of the tail strut. All other regions of foils and struts experience subcavitating flow.

Hydrofoil and strut design provides several air paths to cavity regions. Forced ventilation is provided through tubes to the blunt base of the tail strut and to the blunt trailing edge regions of the diagonal and cruise foil elements of each forward hydrofoil assembly. Air supply for this purpose is obtained from two bleed ports located aft of the compressor section of the gas turbine power plant. Air flow utilized from each port is approximately 0.20 lb/ sec. Natural paths, for air flow from the atmosphere, are also provided. The blunt base of the tail strut extends through the water surface. Similarly, air can flow from the atmosphere to the sides of the afterbody on the forward two struts. At high speed, therefore, only the parabolic forebodies of the forward struts are wetted. The cavities along the afterbody sides can interconnect with cavities on the upper surface of the forward cruise foil elements. A natural air path to the cavity regions of the forward cruise foil elements is also provided along the blunt trailing edges of the diagonal and cruise foils. These blunt bases are connected to each other at the intersection of the two foil elements. In addition, the cavity regions of the cruise foils, at high speed, open directly to the atmosphere since these elements are surface piercing and this forms their primary source of air under cruise conditions. A further possibility for air supply to these regions is through vortices from the foil inboard tips which can extend aft and up to the water surface.

Air from the atmosphere flows to cavity regions with velocity and associated pressure drop. Resultant cavity pressures are thus intermediate between vapor and atmospheric pressures.

A goal of testing at Grumman Aircraft and Dynamic Developments, Inc. is to develop hydrofoil systems which can make a smooth and stable load transition from subcavitating conditions at low speeds to cavity flow conditions at high speeds. Each type of flow is thereby utilized over the speed range where it best affords maximum lift-to-drag ratio. Both surface-piercing and fully submerged foil systems are envisioned which can accomplish this smooth flow transition, and it is expected that several foil arrangements will eventually be tested on the XCH-6.

PERFORMANCE

Curves of estimated vehicle drag and thrust available are plotted vs velocity in Fig. 8. These are typical curves which pertain to current vehicle operation at a gross weight of 2550 pounds. In practice, both thrust available and drag curves can be altered.

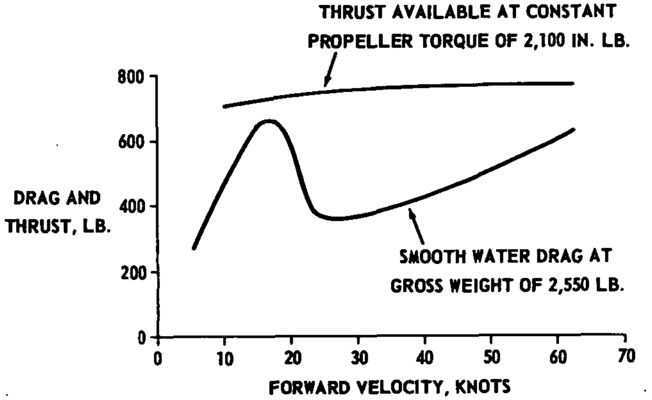

Fig. 8. Estimated smooth water drag and thrust available

Thrust available is dependent upon the size of the shear pin located in the horizontal transmission shafting, aft of the engine gear box. These pins are hollow. The choice of inside diameter and pin material alloy allows selection of maximum transmission and propeller torque. This, in turn, determines available propeller thrust at each forward speed. Normal vehicle operation utilizes a shear pin which is designed to fail when propeller torque reaches 2100 inch-pounds.

Component drag prediction for operation in smooth water has been based upon methods outlined in Refs. 4 and 5. Such prediction appears to be in good agreement with test results obtained to date. The total smooth water drag values given in Fig. 8 can be considered to correspond to normal operation, but the low-speed region can be altered depending upon pilot adjustment of tail foil incidence in pitch with respect to the keel. Minimum takeoff speed, the speed at which the keel just clears the smooth water surface, is approximately 20.0 knots at a gross weight of 2550 pounds.

The propeller was designed to develop 774.0 pounds of thrust at a speed of 62.0 knots and at the maximum rotative speed of 6000 rpm. Predicted propeller efficiency, under these conditions, is 73.9 percent. Associated propeller torque is 2100 inch-pounds.

For operation in smooth water at 60.0 knots, the total drag is estimated to be 660.0 pounds. Only 20.0 percent of this value corresponds to drag due to lift; 8.0 percent is attributed to spray drag; 16.0 percent is due to air drag; the remaining 56.0 percent is due to friction plus pressure drag of wetted elements. This distribution of drag is important when considering vehicles of much larger size with the same cruise speed. Larger craft can be expected to incorporate suitable aerodynamic streamlining, not employed on the XCH-6, and will benefit from considerably reduced friction drag coefficients associated with larger chords and consequently higher Reynolds numbers.

INITIAL TRIALS

Several features of the present configuration have resulted from initial testing.

The nylon liner between the propeller shaft and the propeller hub was provided after an early run wherein the propeller struck a piece of floating debris. The transmission was protected by a shear pin in the drive shaft for conditions of excessive torque from the engine. When excessive torque was suddenly applied from the propeller, however, the inertia of transmission components allowed the bevel gears within the pod to feel the overload prior to shear-pin failure. The result was a tooth failure on one of the bevel gears. Damage to the propeller, consisting of a few nicks on blade leading edges, was very slight and easily corrected by filing.

A reduction in drag, associated with forced air ventilation, was first established by providing air to the blunt base of the tail strut. It allowed the maintenance of given forward velocities with reduced propeller speeds. Provision for forced air supply was then extended to include the blunt base regions of the forward hydrofoils.

During initial trails, a slight porpoising was encountered at approximately 40.0 knots. The oscillation was of constant amplitude, without either build up or decay. It was theorized that ventilation behind the blunt base of the tail strut extended over the sides of the pod near its aft end so as to cause a small decrease in total lift of the tail assembly. This change in lift caused a small increase in vehicle trim and a corresponding increase in pod immersion. At the increased immersion, the flow again reseated on the affected region of the pod, initial lift and trim were restored, and the process would then repeat itself, causing a mild and steady oscillation. A small plate was added on top of the pod and behind the strut so as to limit the extent of the air cavity. This change eliminated further oscillation.

Forward foil design has successfully provided a smooth and stable manner of cavity formation over the cruise foils. It is significant that the vehicle has never experienced adverse roll due to uneven extent of ventilation, one side to the other. Further, it has never experienced abrupt changes in pitch as might be caused if ventilation or flow reseating occurred abruptly. This is true for both smooth and rough water operation, and for running at either a constant heading or during turning maneuvers.

CONCLUSIONS

1. Forced air ventilation, into regions behind the blunt base of a strut or foil, is a practical means of drag reduction.

2. Within the limits of completed testing, predicted propeller and ventilated hydrofoil efficiencies have been confirmed.

3. Ventilated hydrofoil systems can be designed to allow cavity formation in a smooth and stable manner. They offer the elimination of abrupt loss in lift associated with some subcavitating foil systems when ventilation occurs. Complete flow stability has been demonstrated over a wide variety of sea conditions and turning maneuvers.

4. Supercavitating foil sections, as compared to subcavitating types, exhibit a reduced lift curve slope which minimizes incremental lift changes associated with orbital velocities within waves. This feature, together with satisfactory hydrodynamic efficiencies, appears to offer an important field for future development.

ACKNOWLEDGEMENTS

Appreciation is expressed to the Grumman Aircraft Engineering Corp. and to the General Electric Company for freely-given technical assistance and component contribution, to Lear, Incorporated for the donation of a linear actuator, and to the Kaman Aircraft Company for the donation of an oil reservoir and deairation device.

REFERENCES

[1] Tachmindji, A.J., Morgan, W.B., Miller, M.L., and Hecker, R., "The Design and Performance of Supercavitating Propellers," David Taylor Model Basin Report C-807, Feb. 1957

[2] Tachmindji, A.J., and Morgan, W.B., "The Design and Estimated Performance of a Series of Supercavitating Propellers," p. 489 in "Second (1958) Symposium on Naval Hydrodynamics," Washington: Office of Naval Research, 1960

[3] Caster, E.B., "TMB 3-Bladed Supercavitating Propeller Series," David Taylor Model Basin Report 1245, Aug. 1959

[4] "Study of Hydrofoil Seacraft," Vol. I, Bethpage, New York: Grumman Aircraft Engineering Corp. and Dynamic Developments, Inc., Oct. 1958

[5] Johnson, V.E., Jr., "Theoretical and Experimental Investigation of Arbitrary Aspect Ratio, Supercavitating Hydrofoils Operating Near the Free Water Surface," NACA RM L57I16 (NASA, Washington), Dec. 1957

DISCUSSION

H. P. Rader (Vosper Limited, Portsmouth)

With my compliments to Mr. Wennagel and also to Mr. Tulin I should like to make just a few remarks concerning the practical application of supercavitating sections. Recently we have tested two propellers with supercavitating blade sections of wedge-shaped thickness distribution. The efficiency of both propellers under noncavitating conditions was rather poor. On analyzing the results according to the method of the equivalent polar curve as devised by Prof. Lerbs we found that the drag coefficients of the equivalent blade sections were much higher than those of supercavitating sections with quasi-elliptic or elliptic-parabolic thickness distribution. In fact the drag coefficients agreed very closely with values published in Dr. Hoerner's excellent book "Fluid Dynamic Drag." The drag coefficient ratios for various thickness-chord ratios are approximately as follows:

Thickness-chord Ratio	C_D *Wedge*/C_D *Ellipse*
0.04	2.5
0.06	4.0
0.08	5.5
0.10	7.1

When we design supercavitating hydrofoils and propellers we must not forget that the boat fitted with the equipment has to pass through the noncavitating speed range. This is particularly important for hydrofoil boats which have a pronounced hump in their resistance curve at a speed where supercavitating conditions may not be obtainable unless artificial ventilation is used. Even with ventilation the drag coefficients of wedge-shaped sections would be higher than those of quasi-elliptic or elliptic-parabolic sections under noncavitating conditions. I noticed in Mr. Wennagel's interesting paper (or rather in Fig. 8) that at the hump the resistance-displacement ratio of the craft described by him is approximately 0.26, which is rather high.

Marshall P. Tulin

With regard to Mr. Rader's comments on the efficiency of supercavitating sections with blunt bases operating in fully cavitating flow, it is, of course, certainly true that such sections are not particularly efficient because of the blunt base, which causes a drag that is proportional to the square of the base thickness. In fact, it was with some surprise that the

David Taylor Model Basin tests of supercavitating propellers revealed that the efficiency of such propellers at design advance ratio was essentially independent of cavitation number, implying that the efficiency was a little bit less at high cavitation number, that is, under fully wetted conditions, than it was in supercavitating operation, and thus indicating that very little price was being paid because of the drag incurred by the blunt section operating under fully cavitating conditions. With regard to the future, I would not care to speculate on what shapes practical supercavitating foils, designed for high performance craft, will take. Certainly in the case of fully submerged foils, flaps and perhaps other such devices will be included; and I think that we must be patient to see how foil shapes will evolve.

Glen J. Wennagel

In regard to Mr. Rader's comment on the ONR boat, the drag hump during takeoff is due in good part to the foil and strut blunt trailing edges. The design gross weight as stated was 2550 pounds. With a 2100-in./lb shear pin, which corresponds to 200 hp at 6000 rpm, we reach a point where the boat will not take off when the gross weight reaches about 3000 pounds. This is without forced air. If the pilot turns on the air, the reduction in drag is apparent and the boat will take off.

T. G. Lang (U.S. Naval Ordnance Test Station)

My comments are directed toward both Mr. Tulin's paper and Mr. Wennagel's paper.

The development of high-speed hydrofoil craft having surface-piercing hydrofoils or struts requires a detailed knowledge of the effects of air ventilation on hydrodynamic forces. The U.S. Naval Ordnance Test Station has conducted a series of experiments on hydrofoil models in which air was forcibly exhausted through ports in the hydrofoil surface. These experiments were conducted in the high-speed water tunnel at the California Institute of Technology in 1958 and 1959. The objectives of the studies were to investigate the use of forced ventilation for the purposes of control and of improving hydrofoil performance characteristics.

Figure D1 shows a model of one hydrofoil used in the tests in which a spanwise series of small holes can be seen just behind the leading edge. In this study, the chordwise location of the holes was varied and the spanwise length changed.

Figure D2 is a top view of this model mounted in the water tunnel showing air being exhausted through the series of holes, while Fig. D3 is a side view. The air did not spring forward of the exhaust point unless extensive cavitation occurred behind the leading edge or unless the hydrofoil was placed at an angle of attack above its fully-wetted stall angle. Figure D4 is a top view of this model placed at the stall angle of attack. The air is seen to ventilate forward of the holes.

Figure D5 is a top view of another model having the same contour in which a small amount of air is exhausted through a single hole in the upper surface. The angle at which the air diverged outward increased as the angle of attack increased. Figure D6 shows this same model at the same angle of attack but with an increased air-flow rate. It is noted that the sides of the air cavity are more distinct in the latter case and the thin, patchy type of ventilation which was seen in the previous figure has disappeared.

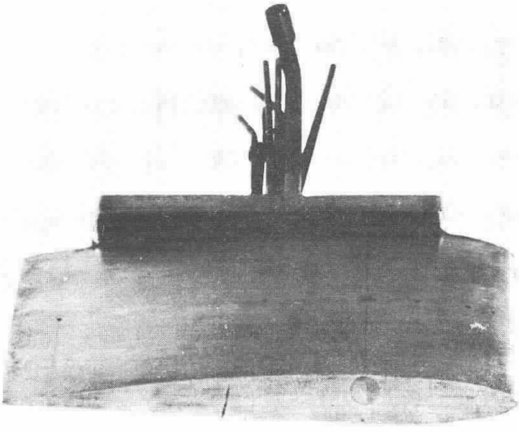

Fig. D1. Hydrofoil model

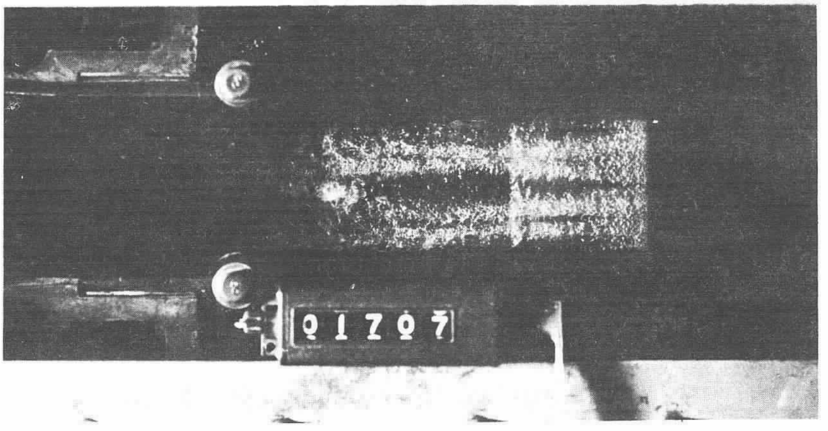

Fig. D2. Top view of the model shown in Fig. D1

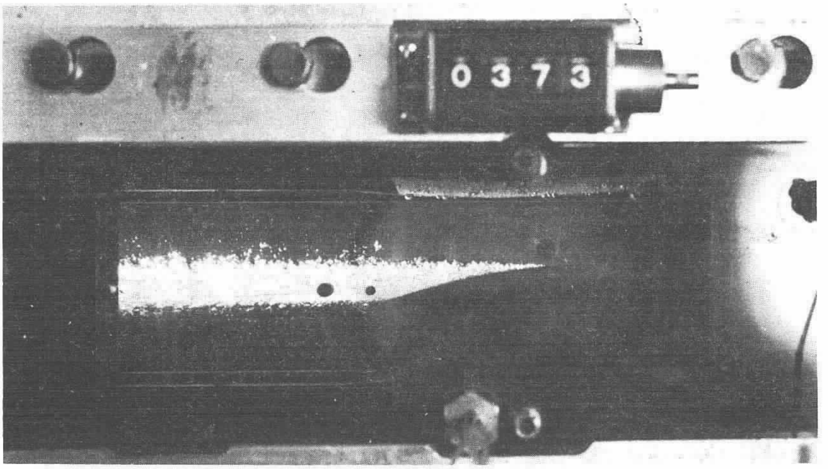

Fig. D3. Side view of the model

Fig. D4. Top view of the model at the stall angle of attack

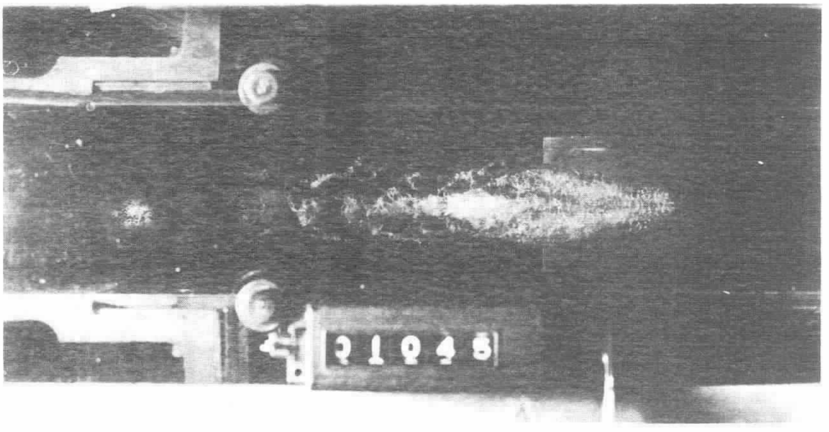

Fig. D5. Top view of a model with a single hole

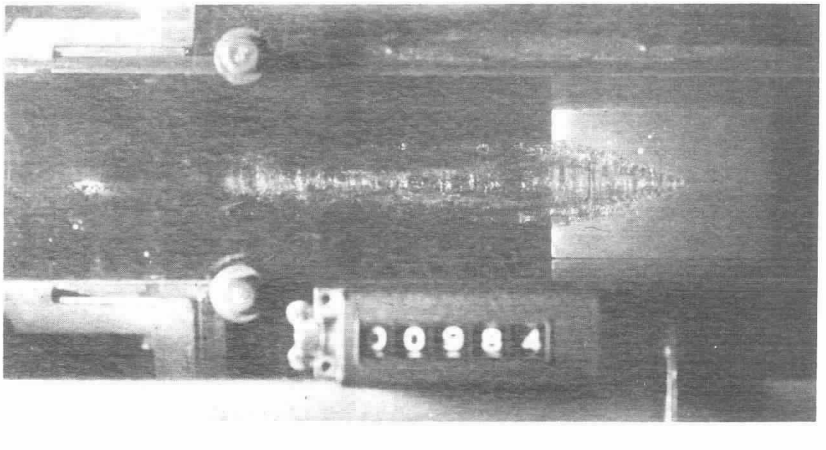

Fig. D6. Same model as Fig. D5 with increased air flow

Figure D7 is a plot of the lift coefficient versus angle of attack. The upper curve refers to fully-wetted flow and the lower curve to vented flow. Note the large decrease in

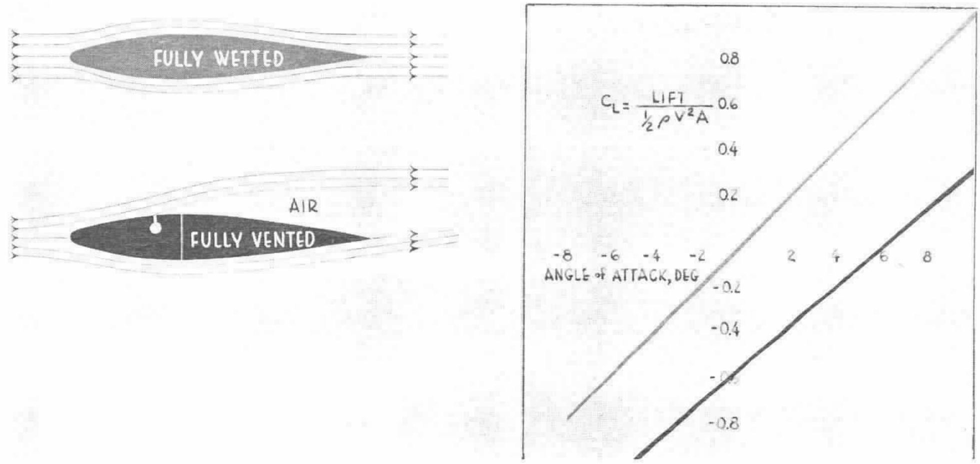

Fig. D7. Lift coefficient of (top curve) fully wetted and (bottom curve) vented hydrofoil

lift when the hydrofoil is forcibly vented. This type of ventilation can be induced by exhausting air through a port at any position on a hydrofoil and therefore may be used as a means of controlling the hydrodynamic forces developed by the hydrofoil. It should also be noted that the slope of the lift coefficient curve is reduced by ventilation. The references cited at the end of this discussion include theoretical work which predicts the lift and drag of two-dimensional hydrofoils of arbitrary shape vented at arbitrary chordwise locations for the case of zero ventilation number. Good agreement is shown with experiment.

Figure D8 shows top and side views of a hydrofoil model having a cambered parabolic cross section wherein air was exhausted through a hole in the trailing edge. The effective

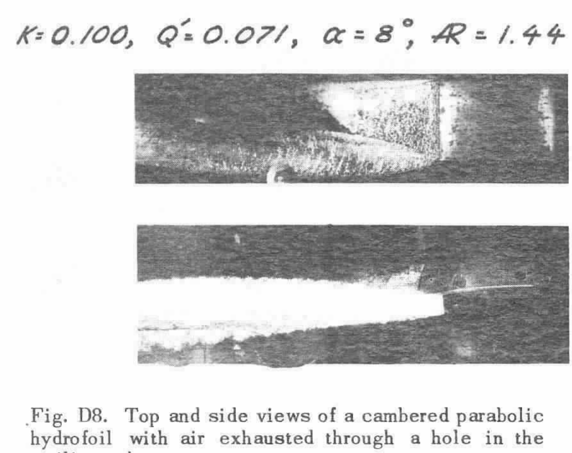

Fig. D8. Top and side views of a cambered parabolic hydrofoil with air exhausted through a hole in the trailing edge aspect ratio in this photograph is 1.44. Note the shape of the air cavity at the tip. As in the previous test series, the air was not seen to ventilate forward of the trailing edge unless a region of separated water existed, such as that caused by stall, extensive cavitation, or boundary layer separation. Figure D9 shows this same hydrofoil in two-dimensional flow with a very small airflow rate. The vortex pattern seen behind the trailing edge disappears when the airflow rate is increased.

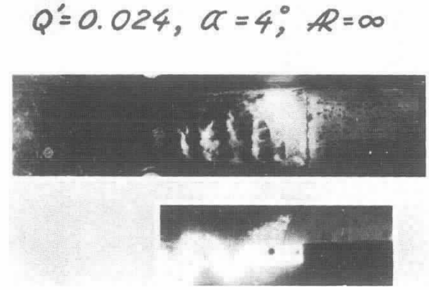

Fig. D9. Hydrofoil of Fig. D8, but with a very small airflow rate

Figure D10 is a plot of the lift-to-drag ratio of the two-dimensional parabolic hydrofoil. The lift-to-drag ratio approaches 25 as the airflow rate increases. Higher ratios could have been obtained if tunnel blockage had not limited the minimum ventilation to K $\geqq$ 0.14.

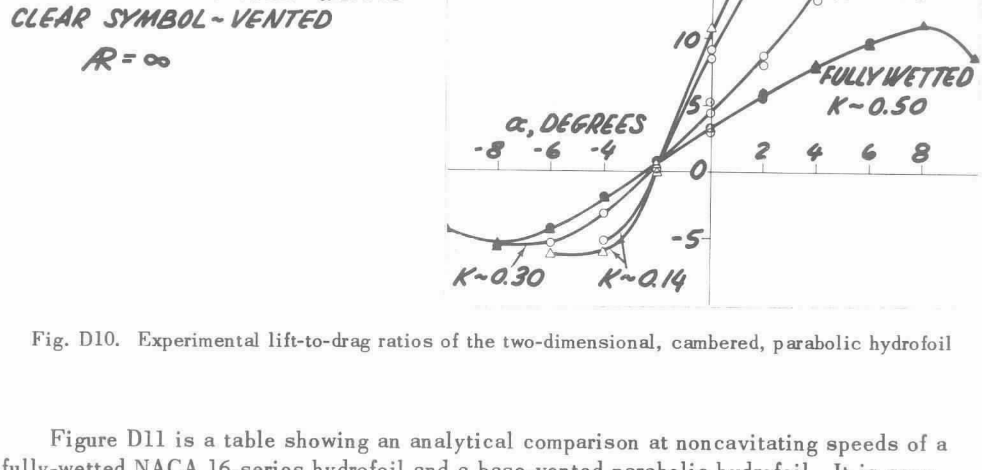

Fig. D10. Experimental lift-to-drag ratios of the two-dimensional, cambered, parabolic hydrofoil

Figure D11 is a table showing an analytical comparison at noncavitating speeds of a fully-wetted NACA 16-series hydrofoil and a base-vented parabolic hydrofoil. It is seen that the cavitation-free speed at the surface may be increased from 20 to over 50 percent by use of the parabolic cross section. The lift-to-drag ratio, however, is decreased.


NACA 16-SERIES


— CAMBERED PARABOLA

	PARAMETERS		RESULTS			
HYDROFOIL	C_L	t/c	C_D	L/D	σ_i	V_{cr} AT WATER SURFACE (KNOTS)
16-SERIES	.50	.15	.0101	49	.67	33
PARABOLA			.0166	30	.32	48
16-SERIES	.25	.15	.0101	25	.51	38
PARABOLA			.0166	15	.16	68
16-SERIES	.50	.10	.0094	53	.55	37
PARABOLA			.0117	43	.32	48
16-SERIES	.25	.10	.0094	27	.39	43
PARABOLA			.0117	21	.16	68
16-SERIES	.50	.05	.0086	58	.44	41
PARABOLA			.0088	57	.32	48
16-SERIES	.25	.05	.0086	29	.28	51
PARABOLA			.0088	28	.16	68

ASSUMPTIONS:

1. TURBULENT FLOW
2. $Re = 2 \times 10^6$, $C_f = .0039$
3. EQUAL C_L AND t/c
4. CIRCULAR ARC CAMBER LINE
5. $K << 1.0$
6. $\alpha = 0°$
7. $AR = \infty$
8. NO SWEEPBACK

Fig. D11. Comparison of hydrofoils having equal lift coefficients and thickness-to-chord ratios

Figure D12 shows a vented hydrofoil which is designed for optimum efficiency. It is constructed by first designing a strut having a thickness distribution and cutoff trailing edge which provides zero cavity drag in accordance with Tulin's linearized cavity theory for zero cavitation number. This strut is then cambered in such a manner that the pressure on the

ASSUMPTIONS: $K = 0$, $\alpha = 0°$, CIRCULAR ARC CAMBER LINE, $AR = \infty$, TURBULENT FLOW, $C_f = 0.0039$

C_L	L/D	σ_i
1.0	128	1.28
.8	114	1.02
.6	96	0.77
.5	86	0.64
.4	73	0.51
.3	59	0.38
.2	42	0.26
.1	23	0.13

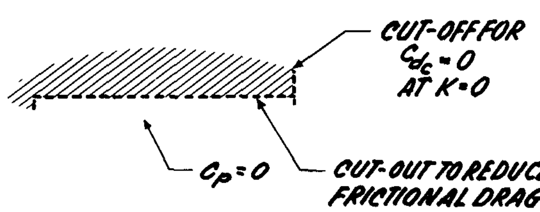

$$L/D = \frac{C_L}{C_f(1 + C_L)}$$

Fig. D12. Base-vented hydrofoil having optimum efficiency lower side is static depth pressure. Once this is accomplished, the lower surface can be ventilated in order to reduce frictional drag. In this manner, all the lift is generated by the upper surface and the lift-to-drag ratio is optimized.

Figure D13 is a theoretical plot of the lift-to-drag ratio versus cavitation number of several hydrofoil shapes. The strength and lift of each of the hydrofoils was assumed to be equal to that of an NACA 16-510 hydrofoil. As the cavitation number was reduced, the chord length and thickness of each hydrofoil was varied to prevent cavitation. The assumptions were two-dimensional flow, a fully turbulent boundary layer, zero angle of attack, circular-arc camber line, and cavity pressure equal to depth pressure.

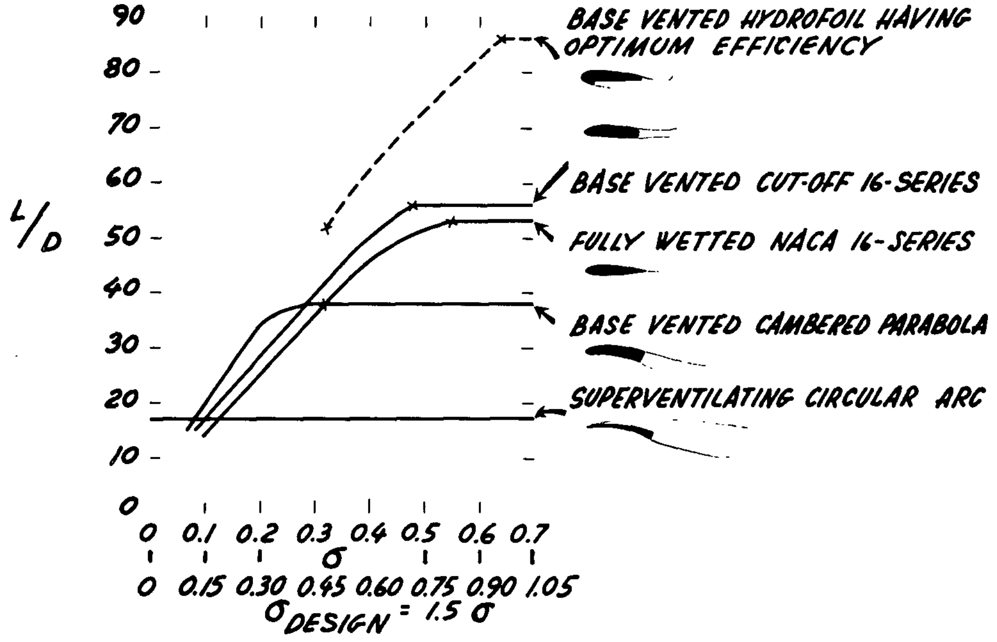

Fig. D13. Comparison of hydrofoils having equal strength and lift

The following reports published at the U.S. Naval Ordnance Test Station include more detailed results of these studies:

1. Lang, T.G., "Base Vented Hydrofoils," NavOrd Report 6606, Oct. 19, 1959
2. Fabula, A.G., "Theoretical Lift and Drag on Vented Hydrofoils for Zero Cavity Number and Steady Two-Dimensional Flow," NavOrd Report 7005, Nov. 4, 1959
3. Lang, T.G., and Daybell, Dorothy A., Smith, K.E., "Water Tunnel Tests of Hydrofoils With Forced Ventilation," NavOrd Report 7008
4. Lang, T.G., and Daybell, Dorothy A., "Water Tunnel Tests of a Base-Vented Hydrofoil Having a Cambered Parabolic Cross Section," NavWeps Report 7584, Oct 10, 1960
5. Fabula, A.G., "Application of Thin Airfoil Theory to Hydrofoils With Cut-Off, Ventilated Trailing Edge," NavWeps Report 7571, Sept. 13, 1960

Marshall P. Tulin

We should all thank Mr. Lang of the Naval Ordnance Test Station for presenting us with his recently obtained experimental information on base- and side-ventilated foils. Work of this kind is most important to continue. I might perhaps mention at this time that the idea of using a fully-wetted but base-ventilated hydrofoil for high-speed operation was, to the best of my knowledge, originated at the Langley Laboratory of the NASA by Mr. Virgil E. Johnson, Jr. These foils are very promising in certain respects, but are also probably very sensitive, cavitation wise, to angle of attack. As was mentioned in the paper, we believe that supercavitating foils intended for use on seagoing boats must be capable of operating without cavitation under a reasonable range of design angles of attack; that range may be larger than is possible with fully-wetted, base-ventilated, parabolic foils.

W. Graff (Versuchsanstalt für Binnenschiffbau, Duisburg, Germany)

The project of a full-cavitating hydrofoil is a proposal of mine made 24 years ago. About 12 years ago I constructed and tested such a boat. The boat was driven by an air-screw of 800 hp. The system of foil was somewhat similar to that shown by Mr. Wennagel and had forward foils piercing the surface and a full-submerged foil aft. The trials of the boat raised serious difficulties. Running on smooth water with full-cavitating foils we got self-excited heaving and pitching oscillations, known as porpoising, such that it was impossible to reach the full speed. Unfortunately, I could not finish these trials. The calculations made on this matter seemed to show that the distance of the foils on high speed was the most important factor in this problem. It was of interest to hear that Mr. Wennagel also observed these phenomena and that he was able to eliminate them.

* * *